IEEE Access
Multidisciplinary | Rapid Review | Open Access Journal
SPECIAL SECTION ON ADVANCED ENERGY STORAGE TECHNOLOGIES AND THEIR APPLICATIONS

Received March 20, 2018, accepted April 16, 2018, date of publication April 20, 2018, date of current version May 16, 2018.

Digital Object Identifier 10.1109/ACCESS.2018.2828802

Multi-Objective Optimal Design of Permanent Magnet Synchronous Motor for High Efficiency and High Dynamic Performance

GUO HONG, TIAN WEI, AND XIAOFENG DING
School of Automation Science and Electrical Engineering, Beihang University, Beijing 100083, China
Corresponding author: Xiaofeng Ding (dingxiaofeng@buaa.edu.cn)

This work was supported in part by the National Natural Science Foundation of China under Project 51407004 and in part by the Aeronautical Science Foundation of China under Grant 20162851016.

ABSTRACT There is a strong demand for the research of electric vehicles (EVs) in automotive industry, because of an increased concern of the energy depletion and environmental pollution problems caused by oil-fueled automotive. The traction motor drive system is one of the core components of EVs, and a motor with superior dynamic performance and high efficiency could significantly reduce energy consumption and improve riding comfort of EVs. Therefore, in order to achieve high dynamic performance and high efficiency of permanent magnet synchronous motor (PMSM), a multi-objective optimization design method for PMSM based on the artificial bee colony algorithm was proposed in this paper. First, based on the magnetic field analytical model of PMSM, the analytical expressions of the key parameters were deduced, namely, mechanical time constant and electrical time constant. Second, the efficiency and electrical and mechanical time constant were defined as optimization objectives. Third, the efficiency and dynamic performance of the original motor and optimized motor were compared applying the finite-element analysis. Furthermore, one prototype machine was manufactured according to the results of optimization. The dynamic performance and efficiency of the prototype had been tested. The experiments show confident results that the efficiency increased about 1% and the mechanical time constant reduced to 31.4% of initial value.

INDEX TERMS Parameter sensitivity, artificial bee colony algorithm, efficiency, dynamic performance.

I. INTRODUCTION

DUE to the awareness of energy and environmental issues, the traditional automotive industry is developed towards electric transformation [1]. Lots of countries and major automobile manufacturers have invested heavily in the research of EVs. The traction motor system is one of the core components of EVs, and a high efficiency motor can maximize the energy saving of EVs [1], [15]. At present, the operation range, manufacturing cost and rapid acceleration capability have become the key problems restricting the development of EVs [2], [23]. However, efficient motor and drive technology can largely compensate for the shortage of low energy density of batteries. Therefore, the use of efficient motor and drive system is an important direction of the development of EVs.

EVs acceleration time on the highway is an important index to evaluate the dynamic performance. And shorter acceleration time means higher safety and more riding comfortable. In urban traffic, because of the large flow of people, traffic lights, EVs often need start and stop frequently. If the acceleration time of EVs in urban is longer, the possibility of traffic congestion would be greater and traffic accidents would be occurred [2]. Therefore, the requirements for the dynamic performance of EVs traction motor are much more important.

From the above descriptions, it is known that both efficiency and dynamic performance are important for the traction motor in EVs. Compared with other motors, permanent magnet synchronous motor (PMSM) shows many advantages such as high efficiency, high power density and high dynamic performance, etc. It is widely used in EVs in the latest years [3].

The PMSM losses could be divided into several parts: copper loss, iron loss and wind friction loss, etc. [4], [22]. And both copper loss as well as iron loss could be decreased by the optimization of PMSM drive system. At present, the research on the efficiency of PMSM traction system in EVs is mainly focused on two aspects: One is an efficiency optimal design for the motor. By optimizing the size of the motor and using high-performance materials, the efficiency of the motor could be improved. The ratio of inner diameter to out diameter of stator is optimized in order to reduce the motor iron loss and

copper loss [5], [6]; the other one is an efficiency optimal control strategy for the motor system. By adopting appropriate control strategy, the current consumption of the motor is minimized, and the overall efficiency of the motor drive is enhanced [4].

However, the adjustment of the ratio of inner diameter to outer diameter of stator will seriously affect the rotor outer diameter. Due to the outer diameter of stator is constant in most case, the increase in ratio of inner diameter to outer diameter of stator will lead to the increase of the inner diameter of stator as well as the out diameter of rotor. Meanwhile, the inertia of rotor is proportion to the biquadrate of the rotor outer diameter, which means a small increase in the outer diameter of the rotor will result in a distinct increase in the rotor inertia [7]. When the output torque of the motor is constant, the increase of the inertia of rotor will cause the acceleration of the motor to be reduced and degrade the dynamic performance of the motor. Therefore, in order to enhance both the efficiency and dynamic performance of the EVs traction motor, it is necessary to investigating the optimization method employing multi-objective optimization algorithm.

To achieve high dynamic performance, many strategies can be adopted in motor design. First, the motor can be designed with low rotor inertia through optimizing the design of rotor structure such as holing the core of rotor [8]. Second, many special structures of magnets such as magnet of prismatic shape [9] and Halbach array [10] can be adopted and making the yoke of rotor thin enough to reduce the inertia of rotor. Both of these methods are to make the inertia of rotor to small and enhance the dynamic performance of motor. However, the dynamic performance of motor is not only related to the inertia of motor. The torque of motor is also important to the dynamic performance. The high ratio of torque to the inertia of rotor means a high acceleration. Therefore, a motor designed with high ratio of torque to the inertia of rotor could lead to a great improvement in dynamic performance [7]. Because the mechanical time constant consists of the ratio torque coefficient to inertia of motor [20], the mechanical time constant could be optimized instead of the ratio for the better dynamic performance.

However, the torque is limited by the response of current. The model of motor is one circuit consists of inductances and resistances. Due to the influence of inductance, the response of current may lag the input controlled voltage and degrade the acceleration. Therefore, the response of current should be considered in the process of optimizing the dynamic performance of motor. As the electrical time constant is defined as the value of inductance divided by resistance, the electrical time constant can be used to manifest the response of current.

Therefore, a novel method is proposed in this paper to improve the dynamic performance of motor, which is based on reducing the values of both the electrical time and the mechanical time constant. The method is not only considering the ratio of torque to inertia through mechanical time constant but also considering the influence of current response through electrical time constant.

In addition, ABC algorithm is a new heuristic optimization algorithm, which simulates the behavior of bees in nature [17]. Compared with other classical optimization method, ABC algorithm is faster and more efficient [18]. Therefore, the ABC is used to optimize the design of this motor for high performance.

In this paper, in order to improve the efficiency and dynamic performance of a PMSM used in EVs, a novel multi-objective optimal method based on ABC was proposed. First, the expressions of efficiency, and mechanical and electrical time constant were deduced, which were the functions of the parameters of the motor, and selected as the optimal objectives. The related parameters of the optimal objectives were defined as optimal variables, such as stator inner diameter, airgap, teeth width, teeth height, etc. Second, thanks to the advantage optimal method ABC, the optimized motor was obtained. Third, both the efficiency and dynamic performance of the original motor and the optimized one were analyzed through 2D finite element simulations and compared comprehensively. Furthermore, the prototype of the optimal motor was manufactured, and the efficiency and dynamic performance of the optimized motor were tested.

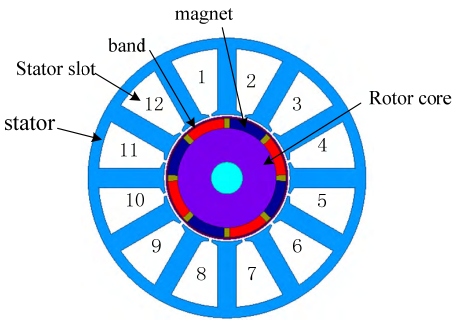

FIGURE 1. The 2 D model of initial electrical machine.

II. MOTOR EFFICIENCY AND DYNAMIC RESPONSE CONSTRAINTS

A. ELECTRICAL MACHINE MODEL

The original motor is a surface mounted PMSM (SPMSM) with 3 phases, 12 slots, 10 poles and non-overlapped concentrated windings. Thanks to the shorter lengths of the end windings, the non-overlapped concentrated winding shows many advantages such as high efficiency, high power density and compactness construction [11]. Hence, many electrical machines with this winding structure are widely used in electrical transportation. Compared with the interior PMSM, the outer diameter of rotor in SPMSM can be downsized enough, which is helpful to reduce the rotor inertia and improve the dynamic performance of the motor. Therefore, the rotor of the original motor implements the surface mounted permanent magnets with radial magnet flux. The structure of the original motor is presented in Figure 1. And the main parameters of the original motor are listed in Table 1.

TABLE 1. Main parameters of the original motor.

Parameter	Value	Parameter	Value
Input voltage: (Vdc)	270	Airgap length (mm)	1
Output power (kW)	20	Magnet thickness (mm)	4.5
Rated speed (rpm)	6000	Embrace	0.85
Rated torque (N.m)	20	Current density ($A/mm^{2)}$	6.3
Pole pairs	4	Efficiency	94.5
Stator out diameter (mm)	132	Stator Slot Fill Factor	63%
Stator inner diameter (mm)	70	Armature phase Resistance : Ω	0.03588
Stator core length (mm)	140	D-Axis Inductance (mH)	0.86
Tooth width (mm)	9	Moment of inertia ($kg.m^2$)	0.00113
Tooth tip height (mm)	1	Electrical constant tim e: ms	23.9686
Tooth open width (mm)	1.5	Mechanical constant time: ms	0.2487
Slot height (mm)	28		

B. DYNAMIC PERFORMANCE ANALYSIS OF PMSM

Taking the rotor coordinates (d−q axes) of the motor as reference coordinates, the voltage balance equation of PMSM can be described as follows [12]:

$$\begin{cases} U_{\mathrm{d}} = L_{\mathrm{d}}\dfrac{di_{\mathrm{d}}}{dt} + Ri_{\mathrm{d}} - \dfrac{P}{2}\omega_{\mathrm{m}}L_{\mathrm{q}}i_{\mathrm{q}} \\ U_{\mathrm{q}} = L_{\mathrm{q}}\dfrac{di_{\mathrm{q}}}{dt} + Ri_q + \dfrac{P}{2}\omega_{\mathrm{m}}L_{\mathrm{d}}i_{\mathrm{d}} + \dfrac{P}{2}\omega_{\mathrm{m}}\Psi_{\mathrm{f}} \end{cases} \tag{1}$$

where

U_{d} :d-axis voltage (volt),
U_{q} :q-axis voltage (volt),
i_{d} :d-axis current (A),
i_{q} :q-axis current (A),
L_{d} :inductance in d-axis (H),
L_{q} :inductance in q-axis (H),
ω_{m} :Mechanical angular velocity (rad/sec),
P :Number of poles,
R :Resistance of motor(ohm)
Ψ_{f} :Flux of permanent magnetic (Wb).

The torque and torque balance equation of PMSM can be described as follows:

$$\begin{cases} T_{\mathrm{e}} = \dfrac{P((\psi_{\mathrm{f}} + L_{\mathrm{d}}i_{\mathrm{d}})\, i_{\mathrm{q}} - L_{\mathrm{q}}i_{\mathrm{q}}i_{\mathrm{d}})}{2} \\ \dfrac{d\omega_{\mathrm{m}}}{dt} = \dfrac{T_{\mathrm{e}}}{J} - \dfrac{B}{J}\omega_m - \dfrac{T_{\mathrm{L}}}{J} \end{cases} \tag{2}$$

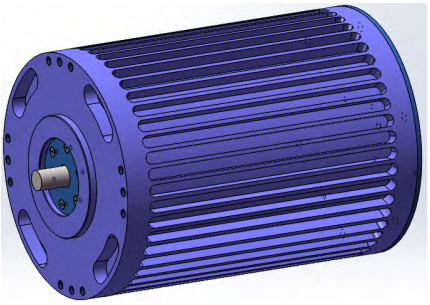

FIGURE 2. 3 D model of initial electrical machine.

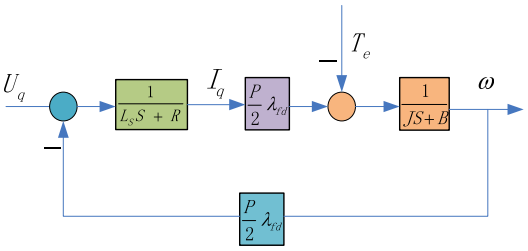

FIGURE 3. The control block diagram.

where

T_{e} :Electromagnetic torque (Nm),
J :Inertia of rotor (kg/m^2),
B :Damping coefficient (Nm/rad/sec),
T_{L} :The torque of Load (Nm).

Usually, the d-axis reference current i_d is set to be $i_{\mathrm{d}} = 0$ in order to approximately eliminate the couplings between angular velocity and currents [13]. If the $i_{\mathrm{d}} = 0$ control strategy is adopted. Then, the electromagnetic torque equation can be simplified to

$$T_{\mathrm{e}} = \frac{P\psi_{\mathrm{f}}i_{\mathrm{q}}}{2} = K_{\mathrm{t}}i_{\mathrm{q}} \tag{3}$$

where K_t is coefficient of torque.

Through Laplace transformation of (1)-(3), the results can be obtained as the following expressions:

$$\begin{cases} \dfrac{i_q(s)}{U_q(s) - \dfrac{P}{2}\omega_m\Psi_f} = sL_q + R \\ \dfrac{d\omega_m}{dt} = \dfrac{K_t i_q}{J} - \dfrac{B}{J}\omega_m - \dfrac{T_L}{J} \end{cases} \tag{4}$$

A transfer function (5) can be obtained by Equation (4). Then, the corresponding control block diagram is descripted in Figure 3.

$$\frac{\omega_{\mathrm{m}}(\mathrm{s})}{U_{\mathrm{a}}(\mathrm{s})} = \frac{K_{\mathrm{t}}}{\mathrm{s}(L_{\mathrm{q}}J\mathrm{s}^2 + RJ\mathrm{s} + K_{\mathrm{t}}K_{\mathrm{e}})} \tag{5}$$

The dynamic performance of motor can be described by two time constants, namely electrical time constant and mechanical time constant [14].

The motor's electrical time constant is the time required for the current to reach 63.2% of its final value when a

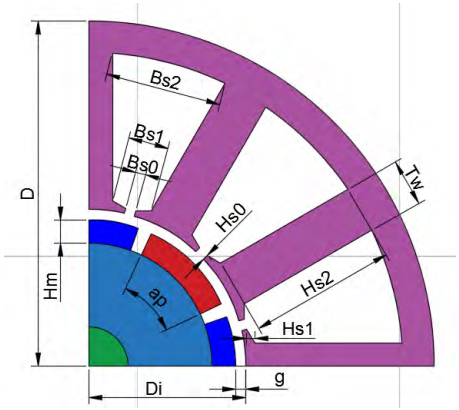

FIGURE 4. One fourth part of motor.

zero source impedance stepped input voltage is applied to a motor maintained in its locked rotor or stalled condition (i.e., $\omega = 0$). The motor's electrical time constant is defined as:

$$\tau_{\mathrm{e}} = \frac{L}{R} \tag{6}$$

The motor's mechanical time constant is given as [14]:

$$\tau_{\mathrm{m}} = \frac{RJ}{K_{\mathrm{e}}K_{\mathrm{t}}} \tag{7}$$

From Equations (6) and (7), it can be seen that the electrical time constant is mainly related to the inductance and resistance, and the mechanical time constant is mainly related to inertia of rotor, resistance, back EMF constant and torque coefficient. Furthermore, the resistance (1), inductance (2), back electromotive force constant (3) and torque coefficient of the motor (4) are closely related to the structure and parameters of the motor. The expressions of each parameter are deduced as follows.

The resistance (1) can be expressed as:

$$R = \rho_{\mathrm{w}}\frac{2NL_{\mathrm{E}}}{A_{01}a_1} \tag{8}$$

where

ρ_{w} :Conductor resistivity,
L_{E} :Average length of half turn,
A_{01} :Cross sectional area of enameled wire,
a_1 :Number of parallel branches.

The inductance includes two parts: the armature inductance and the leakage inductance. It is closely related to the magnetic circuit structure of the motor. The armature inductance is produced by the excitation flux passing through the armature winding. The leakage inductance is caused by the leakage magnetic field of the stator slot, the harmonic magnetic field, the leakage magnetic field of the stator tip leakage, the leakage magnetic field in end winding. The sizes of each part of the initial motor are shown in Figure 4 and the flux of initial motor is shown in Figure 5.

The inductance of the motor (2) can be expressed as:

$$L = L_\sigma + L_{\mathrm{a}} \tag{9}$$

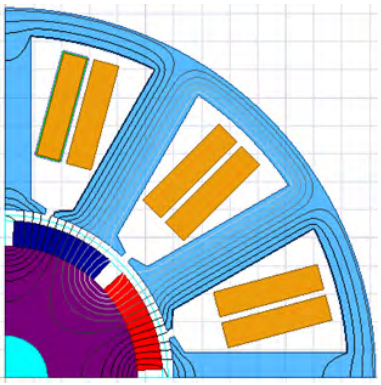

FIGURE 5. Flux line of motor.

where

L_σ :Leakage inductance,
L_{a} :Armature inductance.

The leak inductance of the motor can be expressed as:

$$L_\sigma = L_{\sigma s} + L_{\sigma t} + L_{\sigma end} + L_{\sigma h} \tag{10}$$

where

$L_{\sigma s}$:Leakage inductance in stator slot,
$L_{\sigma t}$:Leakage inductance in top of teeth,
$L_{\sigma end}$:Leakage inductance in winding end,
$L_{\sigma h}$:Harmonic leakage inductance.

The stator slot leak inductance can be expressed as:

$$\begin{cases} q_1 = \dfrac{Q}{2mp} \\ \beta = \dfrac{y}{mq_1} \\ K_{u1} = \dfrac{(6\beta - 1)}{4} \\ K_{l1} = \dfrac{18\beta + 1}{4} \\ \lambda_{u1} = \dfrac{H_{s0}}{B_{s0}} + \dfrac{2H_{s2}}{B_{s0} + B_{s1}} \\ K_1 = \dfrac{H_{s2}}{B_{s2}} \\ K_2 = \dfrac{B_{s1}}{B_{s2}} \\ C_{L1} = \dfrac{1}{3} - \dfrac{1-K_2}{4}\left[\dfrac{1}{4} + \dfrac{1}{3(1-K_2)} + \dfrac{1}{2(1-K_2)^2} + \dfrac{1}{(1-K_2)^3} + \dfrac{lnK_2}{(1-K_2)^4}\right] \\ \lambda_{l1} = \dfrac{4K_1}{(1+K_2)^2}C_{L1} \\ C_x = \dfrac{2u_0 L_{ef}\left(K_{dp}N\right)^2 \times 10^{-2}}{p} \\ \lambda_s = K_{u1}\lambda_{u1} + K_{l1}\lambda_{l1} \\ L_{ef} = L_1 + 2\delta \\ L_{\sigma s} = \dfrac{2pmL_1\lambda_s}{L_{ef}k_{dp}^2 Q}C_x \end{cases} \tag{11}$$

where

q_1 :Slots per pole of each phase,
y :Coil pitch,
H_{s0} :The height of slot open,
B_{s0} :The width of slot open,
H_{s2} :The height of slot,
B_{s1} :The width of slot,
δ :The length of airgap,
L_1 :The length of stator core,
Q :Number of stator slot,
k_{dp} :The factor of winding.

The leakage inductance in top of teeth can be expressed as:

$$L_{\sigma t} = \frac{15.5mN^2L_1\left(\pi D_i - b_{s0}Q\right)}{4\pi Q\left(g + h_m\right)} \tag{12}$$

where

m :Number of phase
b_{s0} :Width of slot opening
Q :Number of stator slot
h_m :Thickness of permanent magnet
D_i :Inner diameter of stator
g :the length of air gap

The leakage inductance in winding end can be expressed as:

$$L_{\sigma end} = \frac{0.34}{2p}\left(L_E - \frac{0.32\pi D_i}{p}\right) * \frac{15.5N^2L_1 10^{-8}}{\pi} \tag{13}$$

The harmonic leakage inductance can be expressed as:

$$L_{\sigma h} = \frac{mu_0 D_i L_{ef} N^2 10^{-2}}{p^2 k_\delta k_s g} \tag{14}$$

where

u_0 :Permeability of vacuum,
k_δ :The coefficient of airgap,
k_s :Saturation coefficient of magnetic circuit.

The armature inductance can be expressed as:

$$\begin{cases} \tau = \frac{\pi D_i}{Q} \\ L_a = \dfrac{2mu_0(NK_{dp})^2\tau L_{ef}10^{-2}}{\pi^2 pk_s(k_\delta g + \frac{h_m}{m_{ur}})} \end{cases} \tag{15}$$

where

K_{dp} :Stator winding factor,
m_{ur} :The relative reversion-permeability.

Then the inductance of the motor(2) can be described as follow

$$\begin{aligned} L &= L_\sigma + L_a \\ &= mN^2L_1\left(\frac{15.5\left(\pi D_i - b_{s0}Q\right)}{4\pi Q\left(g + h_m\right)} + \frac{2pmL_1\lambda_s}{L_{ef}k_{dp}^2QN^2}C_x\right. \\ &\quad + \frac{u_0 D_i 10^{-2}}{p^2k_\delta k_s g} + \frac{0.34}{2pm}\left(L_E - \frac{0.32\pi D_i}{p}\right) \\ &\quad \left. * \frac{15.510^{-8}}{\pi}\right) + \frac{2(K_{dp})^{-2}\tau 10^2}{\pi^2 pk_s(k_g g + \frac{h_m}{m_{ur}})} \end{aligned} \tag{16}$$

Then the electrical constant time can be described as follows:

$$\begin{aligned} \tau_e &= \frac{L}{R} \\ &= \frac{mNA_{01}a_1L_1}{2L_E\rho_w}\left(\frac{15.5\left(\pi D_i - b_{s0}Q\right)}{4\pi Q\left(g+h_m\right)} + \frac{4u_0k_s10^2}{Q}\right. \\ &\quad + \frac{u_0D_i10^{-2}}{p^2k_\delta k_s g} + \frac{0.34}{2pm}\left(L_E - \frac{0.32\pi D_i}{p}\right) \\ &\quad \left. * \frac{15.510^{-8}}{\pi}\right) + \frac{2(K_{dp})^2\tau 10^{-2}}{\pi^2 pk_s(k_g g + \frac{h_m}{m_{ur}})} \end{aligned} \tag{17}$$

From the mechanical time constant expression, it can be seen that the mechanical time constant is mainly related to the inertia of rotor, the torque coefficient and the no-load back EMF constant. Furthermore, the torque coefficient, the back EMF constant and the inertia of rotor can be expressed by the structural parameters of motor.

The inertia of rotor can be expressed as follows:

$$\begin{aligned} J = \frac{\pi}{2}L_{ef}\left[\rho_{pm}\left(\frac{D_{i1} - 2g}{2}\right)^4\right. \\ \left. + \left(\rho_{Fe} - \rho_{Pm}\right)\left(\frac{D_{i1} - 2g - 2h_m}{2}\right)^4\right] \end{aligned} \tag{18}$$

where

ρ_{pm} :Permanent magnet density,
g :Length of airgap,
h_m :Thickness of permanent magnet,
ρ_{Fe} :Density of rotor core

The back EMF constant (3) of the motor can be expressed as follows:

$$K_e = \frac{E}{\omega(t)} = \frac{k_{dp}NB_\delta D_{i1}L_{ef}}{\sqrt{2}P} \tag{19}$$

where

k_{dp} :Winding factor,
E :No-load back electromotive force,
N :Number of turns in series,
B_δ :The amplitude of Fundamental magnetic flux density in airgap,
D_{i1} :Stator inner diameter,
L_{ef} :Length of stator,
P :Number of pole pairs.

The torque constant of the motor (4) can be expressed as follows:

$$K_t = \frac{T}{i(t)} = \frac{k_{dp}NB_\delta D_{i1}L_{ef}}{\sqrt{2}P} \tag{20}$$

Hence, the mechanical time constant can be derived from (18)-(20), which is shown as follows:

$$\begin{aligned} \tau_m &= \frac{RJ}{K_eK_t} = \frac{RJ}{K_e^2} = \frac{2\pi\rho_w L_E P^2}{NK_{dp}^2B_\delta^2D_i^2L_{ef}} \\ &\quad \times\left[\rho_m\left(\frac{D_i - 2g}{2}\right)^4 + \left(\rho_{Fe} - \rho_{pm}\right)\left(\frac{D_i - 2g - 2h_m}{2}\right)^4\right] \end{aligned} \tag{21}$$

The electrical time constant and the mechanical time constant manifest the dynamic performance motor. Meanwhile, the two constants can be expressed as the expressions of the motor parameters. The electric time constant is proportional to the number of turns in each phase of the motor, and is also proportional to the reluctance of the magnetic circuit. While, the mechanical time constant of the motor is inversely proportional to the number of turns per phase, and is proportional to the square of the outer diameter of the rotor. The influence of the number of turns per phase on the electrical time constant and the mechanical time constant is contradictory. Therefore, the multi-objective optimization design is needed to optimize the parameters of motor.

C. EFFICIENCY ANALYSIS OF PMSM

The losses of PMSM mainly include three parts: iron loss, copper loss, mechanical loss. The stator iron loss is consists of hysteresis loss, eddy current loss and excessive loss [4]. The copper loss is caused by the Joule heat loss of the winding resistance. The mechanical loss is the friction loss of the bearing and the rotor.

The resistance of each phase R is calculated as follows:

$$R = k_{\mathrm{w}}\rho_{\mathrm{w}}\frac{2NL_{\mathrm{ef}}}{A_{01}a_1} \tag{22}$$

where

A_{01} :Cross-sectional area of wire,
a_1 :The number of parallel branches.

Copper loss can be calculated as follows:

$$P_{\mathrm{cu}} = 2mNR_{\mathrm{cef}}I^2 = 2mN\rho\frac{L_{\mathrm{ef}}}{A_0}I^2 = 2mNIl\rho J = \pi DL_{\mathrm{ef}}\rho AJ \tag{23}$$

where

J :Current density,
Q :Number of slot.

The stator iron loss can be calculated as follows [10]:

$$P_{\mathrm{Fe}} = P_{\mathrm{hys}} + P_{\mathrm{eddy}} + P_{\mathrm{ex}} \tag{24}$$

Then hysteresis loss can be expressed as follows [10]:

$$P_{\mathrm{hys}} = k_{\mathrm{h}}B_{\mathrm{t}}^2 fV_{\mathrm{teeth}} + k_{\mathrm{h}}B_{\mathrm{y}}^2 fV_{\mathrm{yoke}} \tag{25}$$

where

k_{h} :Hysteresis loss factor,
B_{t} :Magnetic flux density in stator tooth,
B_{y} :Magnetic flux density in stator yoke,
f :Synchronous frequency.

The eddy current loss is calculated as follows [10]:

$$P_{\mathrm{eddy}} = k_{\mathrm{e}}B_{\mathrm{t}}^2 f^2 V_{\mathrm{teeth}} + k_{\mathrm{h}}B_{\mathrm{y}}^2 f^2 V_{\mathrm{yoke}} \tag{26}$$

where

k_{e} :Hysteresis loss factor.

The excessive loss is calculated as follows [10]:

$$P_{\mathrm{ex}} = k_{\mathrm{ex}}B_{\mathrm{t}}^{1.5} f^{1.5} V_{\mathrm{teeth}} + k_{\mathrm{ex}}B_{\mathrm{y}}^{1.5} f^{1.5} V_{\mathrm{yoke}} \tag{27}$$

where

k_{ex} :Excessive loss factor.

The $\mathrm{V_{teeth}}$ can be described as follows:

$$V_{\mathrm{teeth}} = H_{\mathrm{s2}}T_{\mathrm{w}}Q \tag{28}$$

where

H_{s2} :The height of tooth,
T_{w} :The width of tooth.

The V_{yoke} can be described as follows:

$$V_{\mathrm{yoke}} = \pi[D^2 - (D_{\mathrm{i}} - H_{\mathrm{s0}} - H_{\mathrm{s1}} - H_{\mathrm{s2}})^2]L_{\mathrm{ef}} \tag{29}$$

where

D :Out diameter of stator,
D_{i} :Inner diameter of stator,
H_{s0} :The height of tooth tip,
H_{S1} :The width of tooth.

According to the output power and losses of PMSM, the efficiency can be determined as follows:

$$Efficiency = \frac{T_{\mathrm{e}}\omega}{T_{\mathrm{e}}\omega + P_{\mathrm{fe}} + P_{\mathrm{cu}}} \tag{30}$$

where

T_{e} :Output torque,
ω :Angular velocity,
P_{fe} :Core loss,
P_{cu} :Copper loss.

III. OPTIMIZATION PROBLEM

A. OPTIMAL VARIABLES AND OPTIMAL OBJECTIVES

In most cases, a traditional multi-objective optimization of PMSM with n objectives, m variables and l constrains can be described as follows:

The design variable is :

$$x = [x_1, x_2, x_3 \ldots x_m], \quad x\epsilon\mathrm{R^m} \tag{31}$$

The boundary of the variable is:

$$x_{\mathrm{i}}^{\mathrm{L}} < x_{\mathrm{i}} < x_{\mathrm{i}}^{\mathrm{U}}, \quad \mathrm{i} = 1, \ldots, \mathrm{D} \tag{32}$$

The design constraints can be defined as follows:

$$K = \left\{g_{\mathrm{i}}(x) \le 0, x\epsilon\mathrm{R^m}\right\} \mathrm{i} = 1, 2, \ldots, \mathrm{l} \tag{33}$$

The objective function can be set as follows:

$$F = \mathrm{Min}\left\{\mathrm{f}_1(x), \mathrm{f}_2(x), \mathrm{f}_3(x), \ldots, \mathrm{f}_{\mathrm{n}}(x)\right\}, \quad x\epsilon\mathrm{R^m} \tag{34}$$

where x is design variable belong to the K, which is formed by $g_{\mathrm{i}}(x)$. F is the objective function.

Both high efficiency and high dynamic performance are our pursuit in EVs. Meanwhile, the dynamic performance is manifested by the electrical and mechanical time constants. Hence, the efficiency, and the electrical and mechanical time

TABLE 2. optimization variable.

Variable	Maximum value	Minimum value
D_i: inner diameter of stator (mm)	80	46
N_p: turns-in-series per-phase	48	16
L_e: length of stator (mm)	210	70
H_g: height of airgap (mm)	2	0.5
T_m: thickness of magnet (mm)	10	2.5
E_m: embrace	1	0.65
W_s: width of slot open (mm)	3	0.5
W_t: width of tooth (mm)	13.5	4.5
H_s: height of slot (mm)	42	14
H_{s0}:height of slot open (mm)	3	0.5

constants are defined as the optimal objectives, which can be specified as the followings:

$$f_1(x) = \max\{\text{efficiency}(x)\}, x \in K(23)$$
$$f_2(x) = \min\{\text{electrical constant time}(x)\}x \in K$$
$$f_3(x) = \min\{\text{mechanical constant time}(x)\}x \in K \quad (35)$$

According to Equations (17)(21)(30), the electrical time constant, mechanical time constant and efficiency are dependent on the parameters of the motor, such as inner diameter of stator, the length of stator, height of airgap, thickness of magnet, embrace, width of slot open, width of tooth, height of slot ,and height of slot open. Hence, the above parameters are defined as optimal variables in this paper. The range of each variable is listed in Table 2. In order to analyze the influence of the optimized variable of the motor on the optimized objectives, the variation of efficiency, and the mechanical time and electrical time constant in terms of stator diameter and airgap are shown in Figures 6-8.

The variation of rotor inertia with D_i and H_g is shown in Figure 6 (a). And the other parameters are set as constant values. It's known that the increase of D_i will lead to the increase of rotor outer diameter. As a result, the rotor inertia of motor will increase. Hence, the rotor inertia increases as D_i increases, while the rotor inertia decreases as H_g boots shown in Figures 6 (a), 7 (b) and 8 (a). The increase ofH_g will make the outer diameter of rotor becoming smaller that will lead to a reduce in inertia of rotor. Hence, the inertia of rotor decreases as H_g increase as shown in Figures 6 (a) and 8 (a).

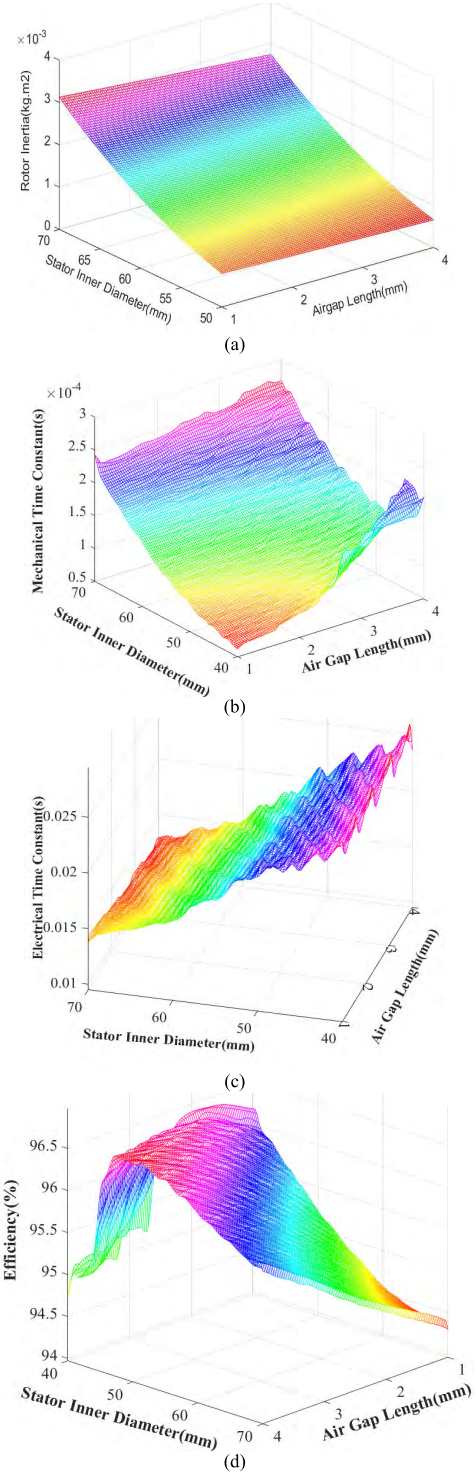

FIGURE 6. The variations of rotor inertia, efficiency, electrical time constant and mechanical time constant with stator inner diameter and air gap length. (a) Variation of rotor inertia with stator inner diameter and air gap length. (b) Variation of mechanical time constant with stator inner diameter and air gap length. (c) Variation of efficiency with stator inner diameter and air gap length. (d) Variation of electrical time constant with stator inner diameter and air gap length.

The number of conduct per slot is discrete. When the back-electromotive force and the flux density in airgap are constant, the increase of D_i will lead to the decrease of

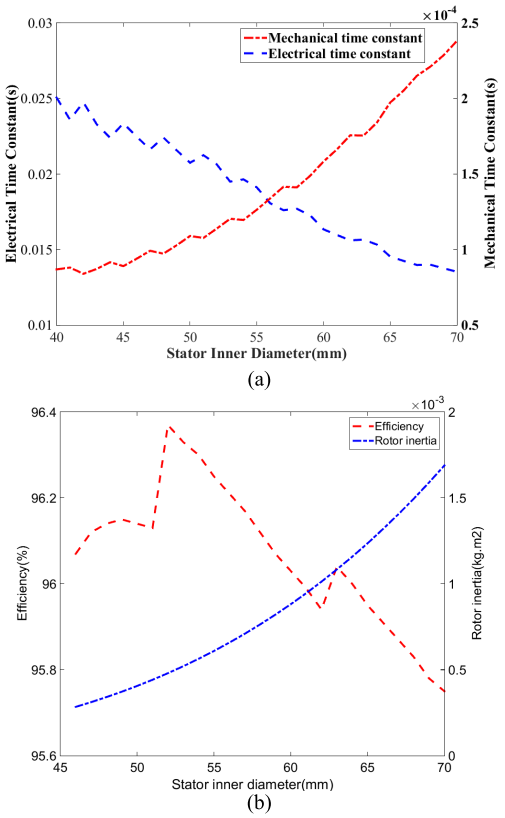

FIGURE 7. The variations of the mechanical time constant electrical time constant, rotor inertia and efficiency with stator inner diameter: (a) Variation of mechanical time constant and electrical time constant with stator inner diameter. (b) Variation of electrical time constant with stator inner diameter.

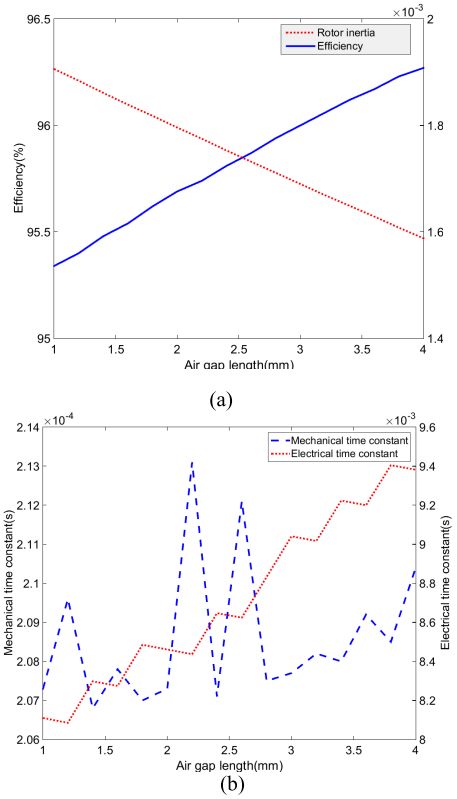

FIGURE 8. The variations of the mechanical time constant electrical time constant, rotor inertia and efficiency with air gap length: (a) Variation of mechanical time constant and electrical time constant with air gap length. (b) Variation of electrical time constant with air gap length.

number of conduct per slot. The inductance of winding (L) is proportional to the square of N_p. However, the resistance of winding (R) is proportional to N_p. Therefore, the increasing of D_i will lead to the decrease of electrical time constant (L/R) as shown in Figures 6 (d) and 7 (a). Because of N_p is discrete, the decreasing waveform of electrical time constant is not smooth.

The inertia of the rotor is proportional to the biquadrate of the outer diameter of rotor. And the D_i is the sum of out diameter of rotor and H_g. Meanwhile, the resistance of winding is proportional to the inner diameter of stator. Therefore, the mechanical time constant increase as the D_i increase shown in Figures 6(b) and 7(a).

The variations of D_i have different effects on the efficiency, mechanical time constant and electrical time constant. One objective is selected a best one may accompany with the deterioration of other objectives. Therefore, a multi-objective optimization design of the motor should be implemented and make a compromise between the optimized objectives.

At present, the traditional method is to assign the weight coefficients to the optimized objectives, and transform the multi-objective problem into a single objective problem, which is consist of compound objective functions [20], [21]. According to this method, a new objective function is defined by combining the objectives with weight coefficients [20]. The new objective function is defined as follows:

$$F = \frac{f_2^i(x) f_3^j(x)}{f_1^k(x)} \tag{36}$$

where f_1 (x), f_2 (x) and f_3 (x) represent efficiency, and electrical time constant and mechanical time constant, respectively. i, j, k are the weight coefficients of objective functions. The weight coefficients are usually assigned to the objective functions based on the importance of the different objectives. Because the dynamic response of the motor speed loop is much worse than the current loop, the weight coefficients selected in this paper are i = 3, j = 4, k = 3. Meanwhile, in order to make a comparative analysis, five representative weight coefficients i = 3, j = 3, k = 3; i = 2.5, j = 5, k = 2.5; i = 2, j = 4, k = 4; i = 2, j = 5 and k = 3 are selected for analysis.

B. ARTIFICIAL INTELLIGENCE BEE COLONY ALGORITHM

Artificial bee colony algorithm is a swarm intelligence evolutionary algorithm inspired by bee foraging mechanism [17]. The algorithm has many advantages such as simple operation, simple control parameters, high search accuracy and strong robustness. In the ABC algorithm, each possible solution is expressed by the position of food source. Any position

of food source can be described as $(X_i = X_{i1}, X_{i2}, \ldots, X_{iD})$, where i is the number of position of food source and D is the number dimension of optimization problem [17]. The value of fitness function is expressed by the quality of food source. The colony of bees can be divided into three parts: employed bees, onlooker bees and scout bees [17]. The employed bees search in the neighborhood of the food sources they memorized before for new food sources and then share the information about the food source with the onlooker bees [18]. The onlooker bees choose one employed bee by the roulette wheel selection and search in local for a new food source around the chosen one. If the food source isn't improved by a predetermined number limit of trials, then that food source will be abandoned by the employed bee, and the employed bees translated to the scout bees and randomly search in global, therefore, this step can effectively avoid local optimal.

The goal of this paper is to enhance both the dynamic performance and the efficiency of motor. Hence, an group of design variables of motor as described in Table 2 (D_i, N_p, L_e, H_g, T_m, E_m, W_s, W_t, H_s, $H_{\mathrm{s}0}$) are defined as the food source. Optimal objectives which consist of efficiency, and the electrical time constant and mechanical time constant as shown in Equation 36 are defined as the quality of food sources. Then the optimization of the efficiency and dynamic performance of the motor is converted into an optimization process based on ABC with ten dimensional vector (D_i, N_p, L_e, H_g, T_m, E_m, W_s, W_t, H_s, $H_{\mathrm{s}0}$. The flowchart of the proposed multi-objective optimization by ABC algorithm is shown in Figure 9. And the details of this method can be described as follows:

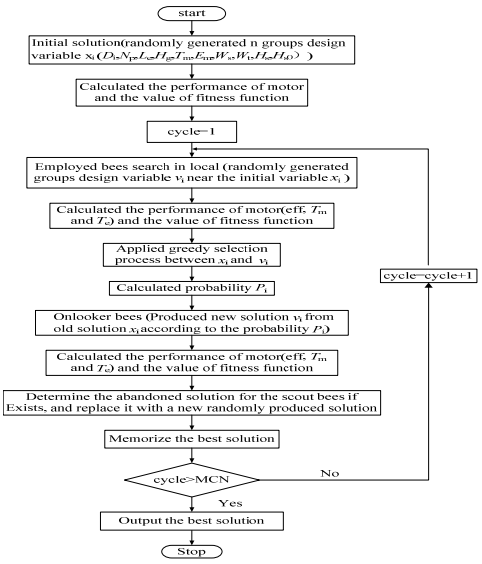

FIGURE 9. Flow chart of ABC algorithm for motor optimal design.

First, initial solution. Randomly generate N groups of design variables, one group includes ten variables, namely D_i, N_p, L_e, H_g, T_m, E_m, W_s, W_t, H_s, $H_{\mathrm{s}0}$, one variable $\mathrm{x_{ij}}$ is shown as follows:

$$x_{ij} = x_{min,j} + \mathrm{rand} \times (x_{max,j} - x_{min,j}) \tag{37}$$

where x_{ij} is design variable as shown in Table 2, $\mathrm{i} \in (0, 1, 2, \ldots, \mathrm{N})$, $\mathrm{j} \in (0, 1, 2, \ldots, 10)$, $x_{min,j}$ is the minimum of one design variable, $x_{max,j}$ is the maximum of one design variable, $\mathrm{rand} \in (0, 1)$ is one random number . N is the number of employed bees, which is selected as 20 in this paper. Then calculated the efficiency, electrical time and mechanical time constant as descripted in Section II in this paper. The fitness function as shown in Equation (36) is calculated.

Second, the employed bees search in local around initial food source. Randomly generated another N-group of design variables v_i (D_i, N_p, L_e, H_g, T_m, E_m, W_s, W_t, H_s, $H_{\mathrm{s}0}$) nearby x_i as follows:

$$v_{ij} = x_{ij} + \partial_{ij} \times (x_{ij} - x_{kj}) \tag{38}$$

where v_{ij} is the new design variable value around the initial design variable x_{ij}. $\partial_{ij} \in (-1, 1)$ is one random number. $\mathrm{k} \in (1, 2, 3, \ldots, 20)$ is one random number and $\mathrm{k} \neq \mathrm{i}$. Then the value of fitness function is calculated. The groupčwhose value of fitness function is better between v_i and x_i, is reserved and the other is abandoned. This process is a local search and the optimal design will be achieved in local.

Third, the onlooker bees select one solution x_i with the corresponding probability value P_i and search for a new candidate v_i nearby x_i. The probability value P_i can be calculated as follows:

$$P_i = \frac{\mathrm{fit}(x_i)}{\sum_{n=1}^{N} \mathrm{fit}(x_n)} \tag{39}$$

Then another group design variable (D_i, N_p, L_e, H_g, T_m, E_m, W_s, W_t, H_s, $H_{\mathrm{s}0}$) is generated by Equation (38). The value of fitness function is calculated and the better solution is reserved between v_i and x_i.

Fourth, if one solution cannot be improved further over the number limit, and it will be abandoned. The employed bees will translate to scout bees and search in global as described by step one. A new group design variable will be generated randomly as shown by Equation (37) to replace the abandoned one. Then the performance of the motor is calculated and the value of fitness function is obtained. This process is global search and can make sure the design is optimized in the global.

Fifth, set the cycle parameter $\mathrm{n} = \mathrm{n} + 1$ and if $\mathrm{n} < \mathrm{n_{max}}$ go back to Step (2), and otherwise the ABC algorithm is stopped and the optimal design is achieved.

C. COMPARISON AND ANALYSIS OF OPTIMIZATION RESULTS

Five sets of objective functions with different weight coefficients are optimized. The value of optimal variables and the value of optimal objectives are shown in Table 3 and Table 4, respectively.

According to the difference of the importance of the optimized target, the different weight coefficients are allocated to the optimized target function. The greater the weight coefficient is, the more important it is to the optimize target.

TABLE 3. Optimal values of variables for different weight coefficients.

Variable (Unit)	i=4, j=4 k=2	i=3 j=4 k=3	i=3 ,j=3 ,k=3	i=2, j=4 k=4	i=2 j=5 k=3	Initial motor
D_i (mm)	46.77	46.55	47.08	46.16	46.46	70
L_e (mm)	146.6	141.6	142	156	129.2	140
H_g (mm)	1.33	1.02	1.05	1.02	1.13	1
W_t (mm)	5.19	6.23	6.51	5.33	5.22	9
H_{s0} (mm)	0.22	0.64	0.59	0.55	0.467	1.5
E_m	0.85	0.77	0.96	0.8	0.7716	0.85
T_m (mm)	8.18	9.48	6.1	5.34	9.076	4.5

TABLE 4. Results of the optimization for different weight coefficients.

Variable	i=4 j=4 k=2	i=3 j=4 k=3	i=3 j=3 k=3	i=2 j=4 k=4	i=2 j=5 k=3	Initial motor
J ($kg.m^2*10^{-3}$)	0.483	0.39	0.485	0.468	0.371	2.252
T_m ($ms*10^{-2}$)	8.71	7.83	9.29	8.09	7.81	24.87
T_e (ms)	17.82	19.9	17.3	22.39	20.95	14.05
eff	94.78	95.5	95.88	95.97	95.3	94.5

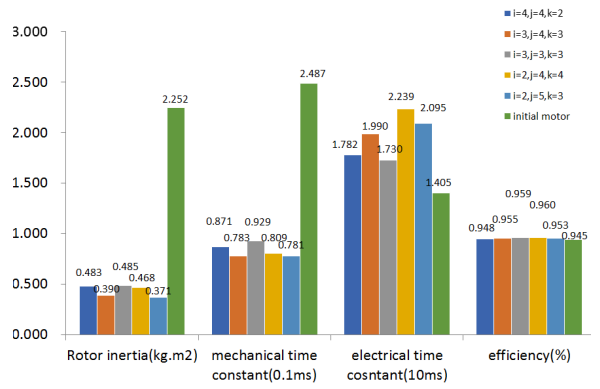

FIGURE 10. Results of different weight coefficients.

The optimization results are shown in Figure 10. Due to the parameter j is the weight coefficient of mechanical time constant, the mechanical time constant is considered as a key objective during the optimization when the weight coefficient is set as i = 2, j = 5, k = 3. Hence, the mechanical time constant is minimal when the weight coefficient is set as i = 2, j = 5, k = 3. In the same condition, the electrical time constant is minimal when the parameter i is set as the maximal value 3. Meanwhile k is the weight coefficient of efficiency. When k is set as 4, the efficiency will be considered as the key objective, the efficiency is the maximum value shown in Figure 10.

Figures 6, 7and 8 indicate that the efficiency of the motor varies little with the value of the optimized variables. Hence, the weight coefficient of the efficiency can be defined as a small value. Meanwhile, the dynamic response of the motor speed loop is much more slow than the current loop, hence, the weight coefficient of the electrical time constant also can be set as a small value. Therefore, the weight coefficients is selected as i = 3, j = 4, k = 3. When the motor is optimized, the efficiency is 1% higher than that of the original one, and the moment of inertia and the mechanical time constant of the motor drop more. The inner diameter of stator is reduced to 46.55mm from 70mm, and then the inertia of rotor is reduced to 17.8% of original motor. Meanwhile, the mechanical time decreases to 31.4% of original motor. The optimization results are particularly obvious.

IV. FINITE ELEMENT SIMULATION ANALYSIS AND EXPERIMENTAL VERIFICATION

The multi-objective optimization design of PMSM is based on the magnetic circuit analysis model, and the analytical expression of each optimization objective is deduced from the magnetic circuit calculation. Due to the value of inductance and loss are influenced by the saturation of the motor, and the saturation degree of each part of the motor is different. The saturation of magnetic circuit in calculation is not enough considered. Therefore, it is necessary to verify the optimized results by finite element simulations.

The 2 D models of both the original and optimized motors are established in Ansoft Maxwell software and compared comprehensively. Figure 11 shows the count plot of magnetic flux density when the machine speed is 6000rpm and the load torque is 10N.m. Due to the width of stator tooth and the length of stator yoke becoming larger after optimization, the density of magnetic in stator tooth and stator yoke reduce. Then the core loss presents a great improvement as shown in Figure 12. The diameters of inner stator become smaller after optimization and then the volume of permanent magnet deduced. Then the eddy current loss which is caused by eddy current decreased as shown in Figure 13. The diameter of inner stator decreasing leads to the torque constant reducing and the input current increasing. Then the copper loss which is mainly caused by the Joule heat loss of the winding resistance increases as shown in Figure 14.The efficiency of the motor have a great improvement after optimization as shown in Figures 14 and 15.

In order to analyze the dynamic performance of the motor, a drive system is set up in Simplorer, which consists of motor model and its controller. And a co-simulation between Simplorer and Maxwell is carried out. The frequency responses of the speed loop of the original motor and optimized motor

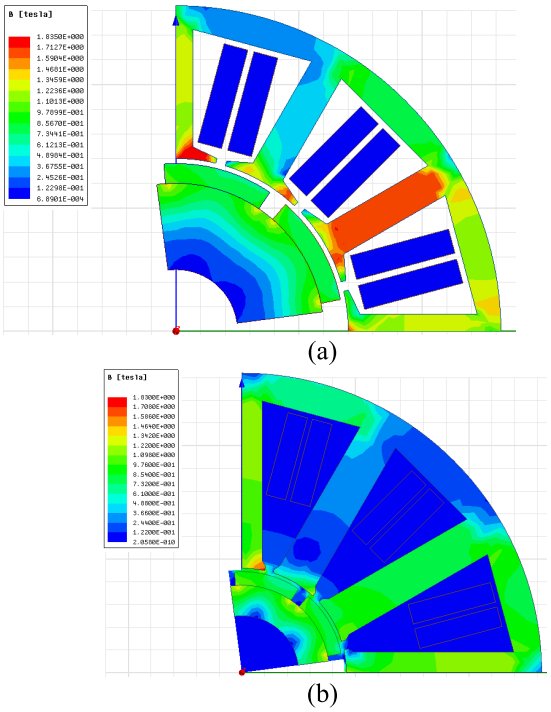

FIGURE 11. The magnetic flux density count plot with full load. (a) The magnetic flux density of initial motor. (b) The magnetic flux density of optimized motor.

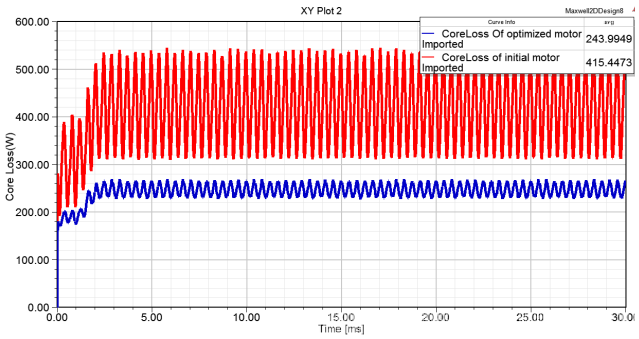

FIGURE 12. The comparison of initial motor core loss and optimized motor core loss.

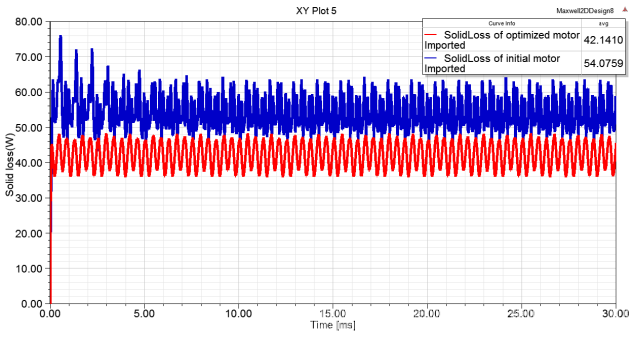

FIGURE 13. The comparison of initial motor solid loss and optimized motor solid loss.

are shown in Figure 16 respectively. It is shown that the frequency response of the optimal motor has improved significantly. The bandwidth of the speed loop increases from

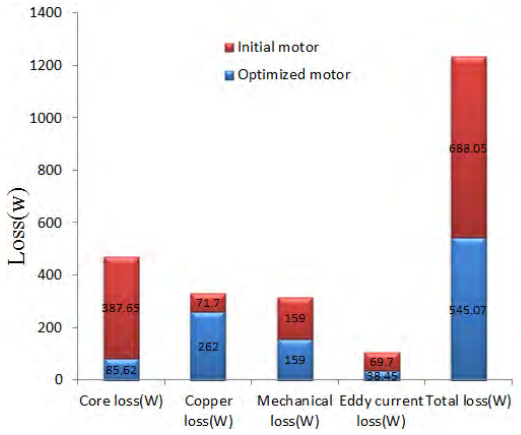

FIGURE 14. The comparison of initial motor loss and optimized motor loss.

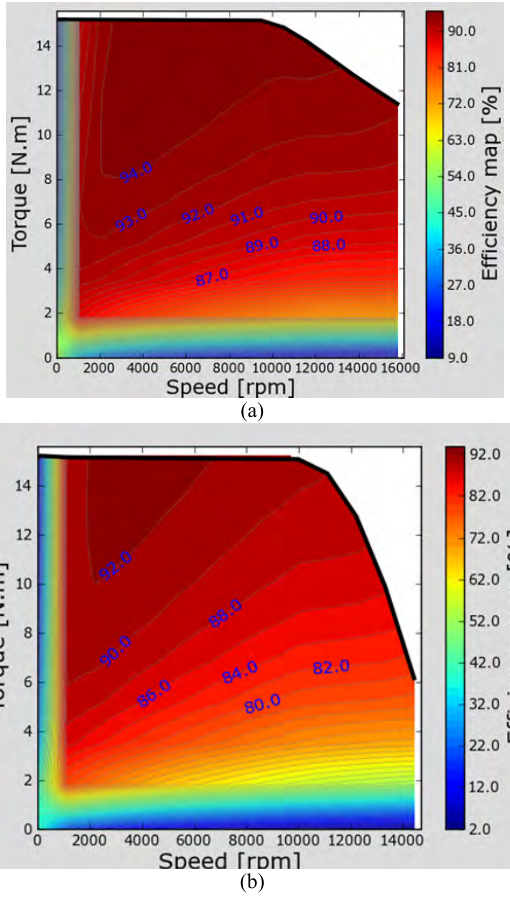

FIGURE 15. The efficiency map of optimized motor and initial motor: (a) Efficiency map of optimized motor. (b) Efficiency map of initial motor.

15HZ to 30HZ. The step response of the original motor's speed loop and optimized motor's speed are shown in Figure 17 and Figure 18. It is shown that the step response of motor has improved significantly. The time length decreases from 62.35ms to less than 21.82ms as the motor reaches a constant speed of 0.632 times. The results indicate that the dynamic performance of the motor has a great improvement and the multi-optimization is effective.

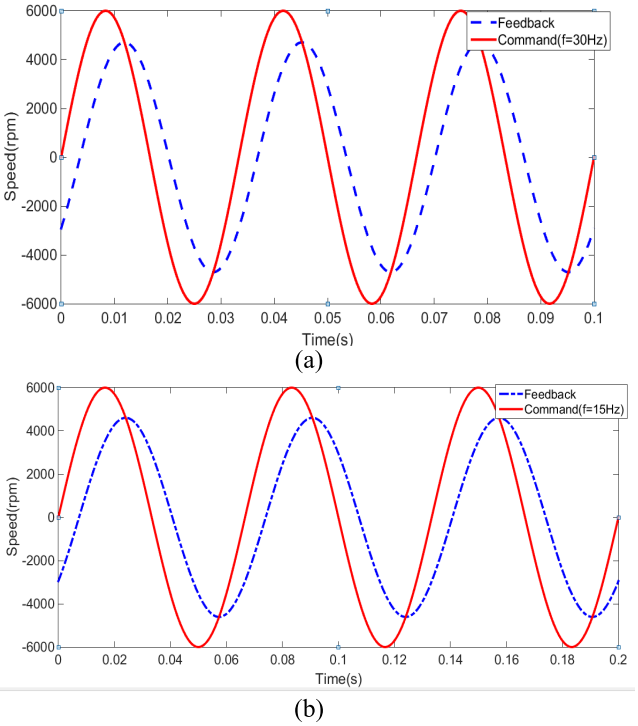

FIGURE 16. The frequency response of motor. (a) The optimized motor frequency response. (b) The initial motor frequency response.

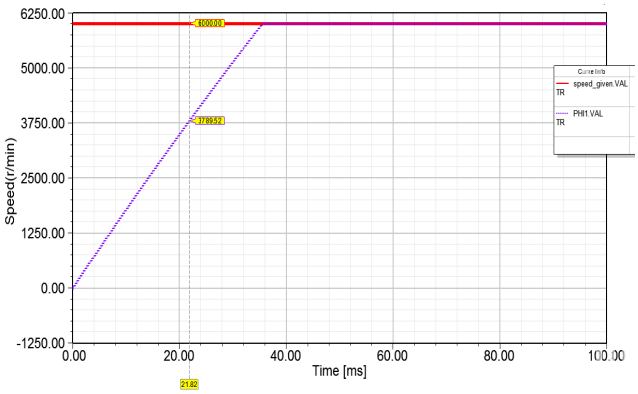

FIGURE 17. Step response of optimized motor's speed loop.

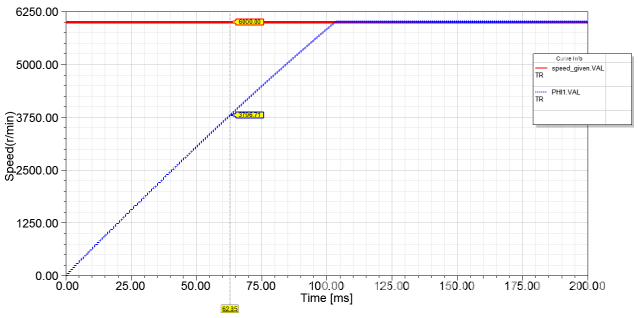

FIGURE 18. Step response of initial motor's speed loop.

As described in section V, the weight coefficients of the final optimization are set as i = 3, j = 4, k = 3 and one prototype machine is manufactured according to the final optimization results. The prototype of machine is shown in Figure 19. To verify the optimization results, the experimental platform based on the designed PMSM is established, including the PMSM, drive controller, dynamometer, power analysis instrument power supply, and CAN bus demonstration. The experimental platform is shown in Figure 20.

FIGURE 19. The prototype of the optimized motor.

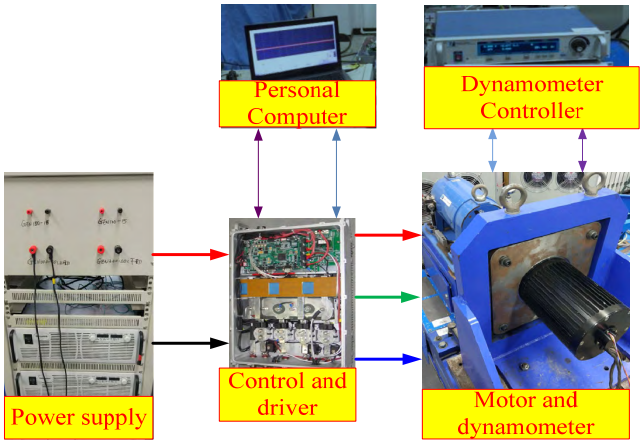

FIGURE 20. The load test bench of motor.

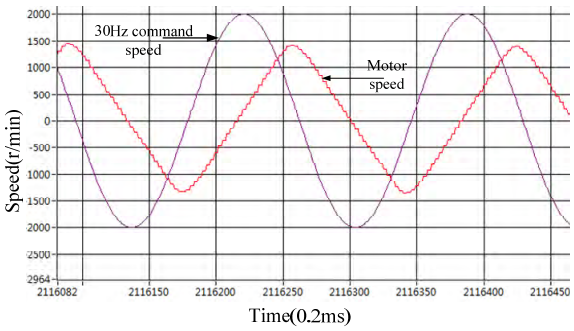

FIGURE 21. Frequency response of motor.

Figures 21 and 22 are the results of dynamic performance test of optimized motor test. As it shown that the time length is 24ms when the motor reaches a constant speed of 0.632 times. This time is longer 3ms than the results of FEA analysis due to the impact of some delays did not considered in analysis such as the time of current sample, time of position sample

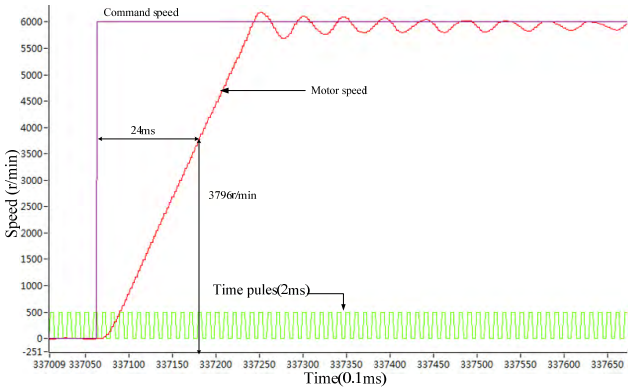

FIGURE 22. Step response of optimized motor test of speed loop.

TABLE 5. Results of efficiency test.

Speed (r/min)	Torque (N.m)	Current (A)	Efficiency (%)
3000	10	25.57	93.14
4000	10	25.63	93.15
5000	10	25.73	93.23
6000	10	25.92	93.56

and so on. From Table 5,we can see that the efficiency of the optimized motor is smaller than the results of FEA analysis. Because the eddy current loss and mechanical loss are hard to calculate accurately. The eddy current loss is influenced by the saturation of the motor, and the saturation degree of each part of the motor is different. The mechanical loss is influenced by various friction factors and the stat of air flow.

V. CONCLUSION

This paper proposed a multi-objective optimal design of a PMSM to achieve high efficiency and high dynamic performance. An analytical model of the motor for magnet circuit calculation was developed. And the expressions of efficiency, mechanical and electrical time constant were deduced, which are the functions of the parameters of the motor. Through the parametric analysis of the motor model, a conclusion was given that the mechanical time constant increases with the increasing of stator inner diameter and with the decreasing of airgap length. However, the efficiency of the motor decreases with the stator diameter increasing and with the decreasing of airgap length.

ABC algorithm was applied to search for the optimal design parameters. As a result, the mechanical time constant and the electrical time constant of the motor were reduced, and the efficiency of the motor was improved. The efficiency of the motor had been increased to 96% from 94.5%. Meanwhile, the mechanical time constant had been reduced to 0.000616 from 0.00218 and the dynamical performance of the motor also had a distinct improvement. The performance of the optimal motor was verified by 2D finite element analysis. Furthermore, one prototype machine was manufactured and the experiments gave further verification.

REFERENCES

[1] J. B. Zhang, C. G. Lu, and C. Q. Li, "The drive control system of micro logistics electric vehicle," *Appl. Mech. Mater.*, vols. 490–491, pp. 1134–1137, Jan. 2014.

[2] L. Ke, Z. Chenghui, and C. Naxin, "Study of high dynamic response strategy for electric vehicle drive system in the high-speed region," *Trans. China Electro-Tech. Soc.*, vol. 22, no. 6, pp. 41–47, Jul. 2007.

[3] C. Zhang, Q. Guo, L. Li, M. Wang, and T. Wang, "System efficiency improvement for electric vehicles adopting a permanent magnet synchronous motor direct drive system," *Energies*, vol. 10, no. 12, p. 2030, 2017.

[4] X. Ding, G. Liu, M. Du, H. Guo, C. Duan, and H. Qian, "Efficiency improvement of overall PMSM-inverter system based on artificial bee colony algorithm under full power range," *IEEE Trans. Magn.*, vol. 52, no. 7, Jul. 2016, Art. no. 8106904.

[5] J. D. Ede, Z. Q. Zhu, and D. Howe, "Optimal split ratio for high-speed permanent magnet brushless DC motors," in *Proc. Elect. Mach. Syst.*, vol. 2. Jun. 2001, pp. 909–912.

[6] Y. Shen, Z. Q. Zhu, and L. J. Wu, "Analytical determination of optimal split ratio for overlapping and non-overlapping winding external rotor PM brushless machines," in *Proc. Electr. Mach. Drives Conf.*, 2011, pp. 41–46.

[7] N. Bianchi, S. Bolognani, and G. Grezzani, "PM motors for very high dynamic applications," in *Proc. IEEE Power Electron. Spec. Conf.*, Jun. 2005, pp. 1332–1338.

[8] S. Huang, G. Wang, J. Gao, K. Huang, and T. Liu "Optimization design of permanent magnet synchronous servo motor with new high dynamic performance," in *Proc. Int. Conf. Elect. Mach. Syst. (ICEMS)*, Beijing, China, Aug. 2011, pp. 1–5.

[9] J. F. Charpentier, "Analytical and numerical study of a new kind of PM brushless motor with trapezoidal EMF for low cost and low inertia applications," in *Proc. IEEE Int. Conf. Electr. Mach. Drives*, May 2005, pp. 1179–1186.

[10] S. Sadeghi and L. Parsa, "Multiobjective design optimization of five-phase halbach array permanent-magnet machine," *IEEE Trans. Magn.*, vol. 47, no. 6, pp. 1658–1666, Jun. 2011.

[11] H. Guo, Z. Wu, H. Qian, and Z. Sun, "Robust design for the 9-slot 8-pole surface-mounted permanent magnet synchronous motor by analytical method-based multi-objectives particle swarm optimisation," *IET Electr. Power Appl.*, vol. 10, no. 2, pp. 117–124, 2016.

[12] Y. Zhang, C. M. Akujuobi, W. H. Ali, C. L. Tolliver, and L.-S. Shieh, "Load disturbance resistance speed controller design for PMSM," *IEEE Trans. Ind. Electron.*, vol. 53, no. 4, pp. 1198–1208, Jun. 2006.

[13] S. Li and Z. Liu, "Adaptive speed control for permanent-magnet synchronous motor system with variations of load inertia," *IEEE Trans. Ind. Electron.*, vol. 56, no. 8, pp. 3050–3059, Aug. 2009.

[14] R. H. Welch, Jr., and G. Younkin, "How temperature affects a servomotor's electrical and mechanical time constants," in *Proc. 37th IAS Annu. Meeting Rec. Ind. Appl. Conf.*, vol. 2. 2002, pp. 1041–1046.

[15] X. Ding *et al.*, "Analytical and experimental evaluation of SiC-inverter nonlinearities for traction drives used in electric vehicles," *IEEE Trans. Veh. Technol.*, vol. 67, no. 1, pp. 146–159, Jan. 2018.

[16] R. Xiong, J. Cao, and Q. Yu, "Reinforcement learning-based real-time power management for hybrid energy storage system in the plug-in hybrid electric vehicle," *Appl. Energy*, vol. 211, pp. 538–548, Feb. 2018.

[17] X. He, W. Wang, J. Jiang, and L. Xu, "An improved artificial bee colony algorithm and its application to multi-objective optimal power flow," *Energies*, vol. 8, no. 4, pp. 2412–2437, 2015.

[18] M. R. Adaryani and A. Karami, "Artificial bee colony algorithm for solving multi-objective optimal power flow problem," *Int. J. Elect. Power Energy Syst.*, vol. 53, no. 1, pp. 219–230, 2013.

[19] M. J. S. Keshayeh and S. A. Gholamian, "Optimum design of a three-phase permanent magnet synchronous motor for industrial applications," *Int. J. Appl. Oper. Res.*, vol. 2, no. 4, pp. 67–86, 2013.

[20] S. Vaez-Zadeh and A. H. Isfahani, "Multiobjective design optimization of air-core linear permanent-magnet synchronous motors for improved thrust and low magnet consumption," *IEEE Trans. Magn.*, vol. 42, no. 3, pp. 446–452, Mar. 2006.

[21] L. Liyi, T. Yongbin, L. Jiaxi, and P. Donghua, "Application of the multiple population genetic algorithm in optimum design of air-core permanent magnet linear synchronous motors," *Proc. CSEE*, vol. 33, no. 15, pp. 69–77, May 2013.
[22] X. Ding, M. Du, T. Zhou, H. Guo, and C. Zhang, "Comprehensive comparison between silicon carbide MOSFETs and silicon IGBTs based traction systems for electric vehicles," *Appl. Energy*, vol. 194, pp. 626–634, May 2017.
[23] R. Xiong, J. Cao, Q. Yu, H. He, and F. Sun, "Critical review on the battery state of charge estimation methods for electric vehicles," *IEEE Access*, vol. 6, no. 1, pp. 1832–1843, Feb. 2018.

GUO HONG received the B.S., M.S., and Ph.D. degrees in electrical engineering from the Harbin Institute of Technology, China, in 1988, 1991, and 1994, respectively. He is currently a Professor with the School of Automation Science and Electrical Engineering, Beihang University, Beijing, China. His research interests include design and control of permanent magnet motor, robust design theory and method of electrical machine, and design theory and method of electrical machines with high reliability.

TIAN WEI received the M.S. degree in electrical engineering from the Guangdong University of Technology, Guangzhou, China, in 2012. He is currently pursuing the Ph.D. degree in electrical machines and electrical apparatus with Beihang University, Beijing, China. His main research interests are the design theory and method of electrical machine with high power density and high efficiency applied in aircraft and electric vehicles.

XIAOFENG DING received the B.S., M.S., and D.S. degrees in electrical engineering from Northwestern Polytechnical University, Xi'an, China, in 2005, 2008, and 2011, respectively. From 2008 to 2010, he was a Visiting Scholar with the University of Michigan–Dearborn, Dearborn, MI, USA.

He is currently an Associate Professor with the Department of Electrical Engineering, Beihang University, Beijing, China, where he is also the Chair in Charge. His research interests include permanent magnet electric machines and their drives based on wide bandgap power devices, such as silicon carbide and gallium nitride devices.